

# Dark Matter in Minimal $U(1)_{B-L}$ Model

Tanushree Basak<sup>1</sup>, Tanmoy Mondal<sup>1,2</sup>

<sup>1</sup>Theoretical Physics Division, Physical Research Laboratory, Ahmedabad 380009, India.

<sup>2</sup>Department of Physics, Indian Institute of Technology, Gandhinagar, Ahmedabad, India.

**DOI:** [http://dx.doi.org/10.3204/DESY-PROC-2014-03/basak\\_tanushree](http://dx.doi.org/10.3204/DESY-PROC-2014-03/basak_tanushree)

We study the  $B - L$  gauge extension of the Standard Model which contains a singlet scalar and three right-handed neutrinos. The third generation right-handed neutrino is qualified as the dark matter candidate, as an artifact of  $Z_2$ -charge assignment. Relic abundance of the dark matter is consistent with WMAP9 and PLANCK data, only near scalar resonances. Requiring correct relic abundance, we restrict the parameter space of the scalar mixing angle and mass of the heavy scalar boson of this model.

## 1 Gauged $U(1)_{B-L}$ Model

The minimal  $U(1)_{B-L}$  extension of the SM [1, 2, 3, 4] contains in addition to SM : a SM singlet  $S$  with  $B - L$  charge +2, three right-handed neutrinos  $N_R^i (i = 1, 2, 3)$  having  $B - L$  charge -1. The assignment of  $\mathbb{Z}_2$ -odd charge ensures the stability of  $N_R^3$  [5, 4] which qualified as a viable DM candidate. Scalar Lagrangian of this model can be written as,

$$\mathcal{L}_s = (D^\mu \Phi)^\dagger D_\mu \Phi + (D^\mu S)^\dagger D_\mu S - V(\Phi, S), \quad (1)$$

where the potential term is,

$$V(\Phi, S) = m^2 \Phi^\dagger \Phi + \mu^2 |S|^2 + \lambda_1 (\Phi^\dagger \Phi)^2 + \lambda_2 |S|^4 + \lambda_3 \Phi^\dagger \Phi |S|^2,$$

with  $\Phi$  and  $S$  as the SM-scalar doublet and singlet fields, respectively. After spontaneous symmetry breaking (SSB) the singlet scalar field can be written as,  $S = \frac{v_{B-L} + \phi'}{\sqrt{2}}$  with  $v_{B-L}$  real and positive. The mass eigenstates ( $H_1, H_2$ ) are linear combinations of  $\phi$  and  $\phi'$  with mixing angle  $\alpha$ . We identify  $H_2$  as the SM-like Higgs boson with mass 125.5 GeV.

The RH neutrinos interact with the singlet scalar field  $S$  through interaction term of the lagrangian:

$$\mathcal{L}_{int} = \sum_{i=1}^3 \frac{y_{n_i}}{2} \overline{N_R^i} S N_R^i. \quad (2)$$

Here we define,  $\lambda_{DM}$  as the coupling between DM candidate and the SM Higgs boson, which is effectively the Yukawa coupling of the  $N_R^3$ . Thus, the mass of dark matter is given by,  $m_{DM} = m_{N_R^3} = \frac{y_{n_3}}{\sqrt{2}} v_{B-L}$ .

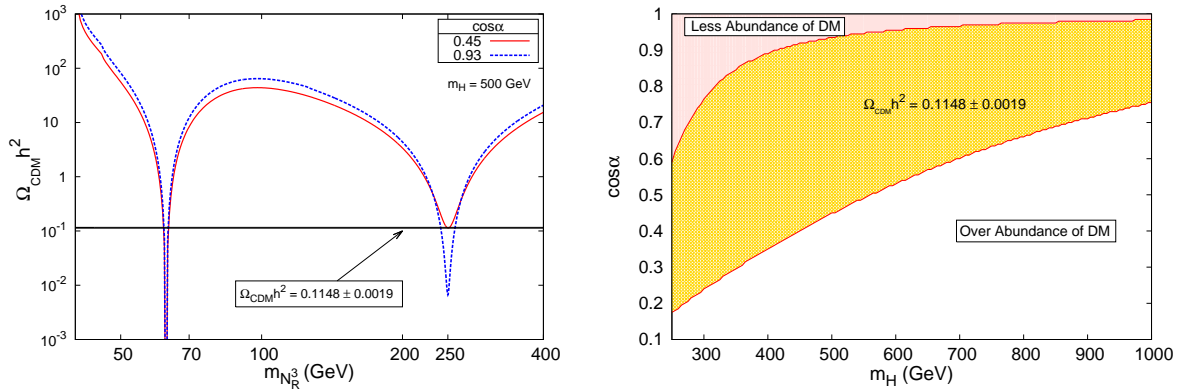


Figure 1: Left : Plot of relic abundance as a function of DM mass for  $m_H = 500$  GeV with specific choices of scalar mixing angle  $\cos \alpha = 0.935$  (blue-dashed),  $0.45$  (red-solid). The straight line shows the WMAP9 value,  $\Omega_{CDM} h^2 = 0.1148 \pm 0.0019$ . Right : Yellow region (in the middle) shows the allowed range of  $\cos \alpha$  and  $m_H$  consistent with correct relic abundance as reported by WMAP9. The above-pink (below-white) region is disallowed due to under-abundance (over-abundance) of dark matter.

## 2 Dark Matter Observations

### 2.1 Relic Abundance

$m_h$	$\Gamma_h$	$v_{B-L}$	$g_{B-L}$
125 GeV	$4.7 \times 10^{-3}$ GeV	7 TeV	0.1

Table 1: Choice of Parameters

A specific set of benchmark values chosen is shown in Table.1. The relic abundance of DM can be formulated as [6],

$$\Omega_{CDM} h^2 = 1.1 \times 10^9 \frac{x_f}{\sqrt{g^*} m_{Pl} \langle \sigma v \rangle_{ann}} \text{GeV}^{-1}, \quad (3)$$

where  $x_f = m_{N_R^3}/T_D$  with  $T_D$  as decoupling temperature.  $m_{Pl}$  is Planck mass =  $1.22 \times 10^{19}$  GeV, and,  $g^*$  is effective number of relativistic degrees of freedom.  $\langle \sigma v \rangle_{ann}$  is the thermal averaged value of DM annihilation cross-section times relative velocity. DM interacts with the SM particles via  $Z'$ -boson and  $h, H$ . But,  $Z'$ -boson being heavy ( $m_{Z'} \geq 2.33$  TeV [7]), the annihilation of DM into the SM particles takes place via  $h$  and  $H$  only. Thus, effectively we

obtain a Higgs-portal DM model.  $\langle\sigma v\rangle_{ann}$  can be obtained using the well known formula [8],

$$\langle\sigma v\rangle_{ann} = \frac{1}{m_{N_R^3}^2} \left\{ w(s) - \frac{3}{2} \left( 2w(s) - 4m_{N_R^3}^2 w'(s) \right) \frac{1}{x_f} \right\} \Big|_{s=(2m_{N_R^3})^2}, \quad (4)$$

where prime denotes differentiation with respect to  $s$  ( $\sqrt{s}$  is the center of mass energy). Here, the function  $w(s)$  depends on amplitude of different annihilation processes,

$$N_R^3 N_R^3 \longrightarrow b\bar{b}, \tau^+ \tau^-, W^+ W^-, ZZ, hh. \quad (5)$$

In Figure. 1 the relic density is plotted against DM mass for two specific choices of scalar mixing angles. The resultant relic abundance is found to be consistent with the reported value of WMAP-9 and PLANCK experiment only near resonance when,  $m_{N_R^3} \sim (1/2) m_{h,H}$ . The reason for the over abundance of DM except at the resonance can be understood in the following way : The annihilation cross-section of DM, being proportional to  $y_{n_3}^2$  (where,  $y_{n_3} = (\sqrt{2}m_{N_R^3})/v_{B-L}$ ), is heavily suppressed due to large value of  $v_{B-L}$ .

Relic abundance near the second resonance depends on the following model parameters (unknown) : scalar mixing angle ( $\alpha$ ), heavy scalar mass ( $m_H$ ) and decay width ( $\Gamma_H$ ). For large mixing angle, the total decay width of heavy scalar is large and hence the annihilation cross-section  $\langle\sigma v\rangle_{ann}$  is less compared to that with minimal mixing scenario. This behavior is observed in Figure. 1, where  $\Omega_{CDM} h^2$  is large for smaller value of  $\cos \alpha$  (at  $m_{N_R^3} \sim (1/2) m_H$ ) and vice-versa. We therefore perform a scan over the entire parameter range of  $m_H$  (300-1000 GeV) and  $\cos \alpha$  (shown in Fig. 1) to find the allowed region consistent with the 9-year WMAP data [9].

## 2.2 Spin-independent scattering cross-section

The effective Lagrangian describing the elastic scattering of the DM off a nucleon is given by,

$$L_{eff} = f_p \bar{N}_R^3 N_R^3 \bar{p} p + f_n \bar{N}_R^3 N_R^3 \bar{n} n, \quad (6)$$

We obtain the scattering cross-section (spin-independent) for the dark matter off a proton or neutron as,

$$\sigma_{p,n}^{SI} = \frac{4m_r^2}{\pi} f_{p,n}^2 \quad (7)$$

where,  $f_{p,n}$  is the hadronic matrix element and  $m_r$  is the reduced mass.

We observe that,  $\sigma_{p,n}^{SI} \propto (\sin 2\alpha)^2 f(m_H)$ , which is maximum at  $\alpha = \pi/4$  (or  $\cos \alpha = 0.707$ ) irrespective of the choice of  $m_H$ . Figure. 2 shows the maximum value of spin-independent scattering cross-section (i.e, with  $\cos \alpha = 0.707$ ) of the DM off proton ( $\sigma_p^{SI}$ ) as a function of DM mass. We observe that the value of the resultant cross-section with two different values of  $m_H$  for the entire range  $6 \text{ GeV} \leq m_{N_R^3} \leq 500 \text{ GeV}$  lies much below the XENON100 and latest LUX exclusion limits. But, as the value of  $m_H$  is increased, the spin-independent cross-section becomes larger at higher values of DM mass and approaches the limits as reported by LUX and XENON100. As shown in Figure. 2, in future XENON1T data might severely restrict the choice of allowed  $m_H$ .

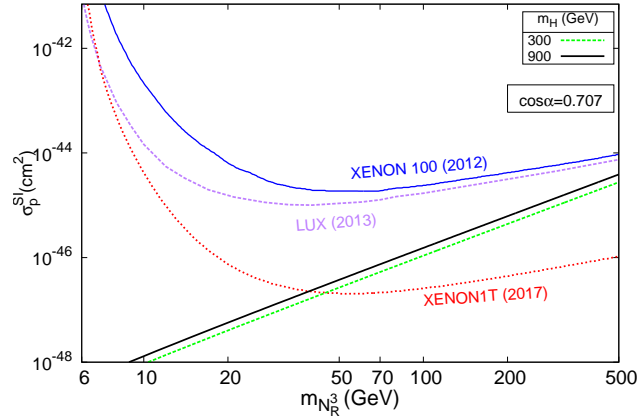


Figure 2: Variation of  $\sigma_p^{SI}$  with  $m_{N_R^3}$  for  $m_H = 300$  GeV (green-dashed) and 900 GeV (black-solid) with  $\cos\alpha = 0.707$ . The blue and violet curves show the bound from XENON100 [10] and LUX [11] data respectively. Red curve shows the projected limits for XENON1T [12].

## Acknowledgements

We would like to thank Joydeep Chakraborty, Partha Konar and Subhendra Mohanty for most useful comments and discussions.

## References

- [1] Shaaban Khalil. Low scale  $B - L$  extension of the Standard Model at the LHC. *J.Phys.*, G35:055001, 2008.
- [2] Lorenzo Basso, Stefano Moretti, and Giovanni Marco Pruna. A Renormalisation Group Equation Study of the Scalar Sector of the Minimal B-L Extension of the Standard Model. *Phys.Rev.*, D82:055018, 2010.
- [3] Lorenzo Basso. Phenomenology of the minimal B-L extension of the Standard Model at the LHC. 2011.
- [4] Tanushree Basak and Tanmoy Mondal. Constraining Minimal  $U(1)_{B-L}$  model from Dark Matter Observations. *Phys.Rev.*, D89:063527, 2014.
- [5] Nobuchika Okada and Osamu Seto. Higgs portal dark matter in the minimal gauged  $U(1)_{B-L}$  model. *Phys.Rev.*, D82:023507, 2010.
- [6] Edward W. Kolb and Michael S. Turner. The Early universe. *Front.Phys.*, 69:1–547, 1990.
- [7] J. Beringer et al. Review of particle physics. *Phys. Rev. D*, 86:010001, Jul 2012.
- [8] Mark Srednicki, Richard Watkins, and Keith A. Olive. Calculations of Relic Densities in the Early Universe. *Nucl.Phys.*, B310:693, 1988.
- [9] G. Hinshaw et al. Nine-Year Wilkinson Microwave Anisotropy Probe (WMAP) Observations: Cosmological Parameter Results. 2012.
- [10] E. Aprile et al. Dark Matter Results from 225 Live Days of XENON100 Data. *Phys.Rev.Lett.*, 109:181301, 2012.
- [11] D.S. Akerib et al. First results from the LUX dark matter experiment at the Sanford Underground Research Facility. 2013.
- [12] Elena Aprile. The XENON1T Dark Matter Search Experiment. 2012.